# ARTICLES

## Far-Infrared Characteristics of ZnS Nanoparticles Measured by Terahertz Time-Domain Spectroscopy

**Jiaguang Han,[†] Weili Zhang,*[,‡] Wei Chen,[§] L. Thamizhmani,[‡] Abul K. Azad,[‡] and Zhiyuan Zhu[†]**

*Shanghai Institute of Applied Physics, Chinese Academy of Sciences, Shanghai 201800, People's Republic of China, School of Electrical and Computer Engineering, Oklahoma State University, Stillwater, Oklahoma 74078, and Nomadics, Inc., 1024 S. Innovation Way, Stillwater, Oklahoma 74074*

*Received: October 12, 2005; In Final Form: December 3, 2005*

The optical and dielectric properties of ZnS nanoparticles are studied by use of terahertz time-domain spectroscopy (THz-TDS) over the frequency range from 0.3 to 3.0 THz. The effective medium approach combined with the pseudo-harmonic model of the dielectric response, where nanoparticles are embedded in the host medium, provides a good fit on the experimental results. The extrapolation of the measured data indicates that the absorption is dominated by the transverse optical mode localized at 11.6 ± 0.2 THz. Meanwhile, the low-frequency phonon resonance of ZnS nanoparticles is compared with the single-crystal ZnS. The THz-TDS clearly reveals the remarkable distinction in the low-frequency phonon resonances between ZnS nanoparticles and single-crystal ZnS. The results demonstrate that the acoustic phonons become confined in small-size nanoparticles.

### I. Introduction

Due to fascinating physical and chemical properties and potential applications in a broad range of disciplines, semiconductor nanoparticles have attracted enormous theoretical and experimental attention during the past two decades.[1−4] Compared to bulk materials, the variation in the properties of nanoparticles arises mainly from the increase in surface-to-volume ratio and drastic change in the electronic structure due to quantum mechanical effects with decreasing particle size. The large surface-to-volume ratio enables the surface atoms in nanoparticles to be bound by weaker forces, which in turn results in a high surface reactivity. The surface effects generally have an extensive influence on the optical spectra. Hence, nanoparticles often have a quite dissimilar optical response from bulk materials.[5−7]

As a wide band gap (3.6 eV) II−VI compound, ZnS is an attractive semiconductor for cathode-ray tube luminescent materials, catalysts, electroluminescence, solar cells, and UV semiconductor lasers. ZnS is also an excellent optical material in the IR and the far-IR regions owing to low absorption; it thus can be used for IR windows and lenses.[8,9] ZnS nanoparticles, which can be synthesized by use of various chemical methods ranging from reverse micelles to polymers, have potential applications in areas such as nonlinear optical devices and fast optical switches.[10−12] They exhibit a strong quantum size effect in the nanometer region. It was observed that ZnS nanoparticles in a very small size range (2−3 nm) often tend to have a hexagonal wurtzite phase.[13] Recently, the nature of vibrations of ZnS nanoparticles has received much attention. The investigation of low-frequency optical characteristics in ZnS nanoparticles is essential to clearly understand their dielectric properties, optical mode behavior, and size effect. The surface optical modes of ZnS nanoparticles have been well characterized in the frequency range of 100−700 $cm^{-1}$.[14] However, due to the spectrum limit, the measurements did not reach the broad terahertz spectral region (<100 $cm^{-1}$, 3 THz). Terahertz time-domain spectroscopy (THz-TDS) is a nonionizing, coherent quasi-optic, and phase-sensitive modality and has been used in the characterization of a wide variety of materials. Some of the prominent phonon resonances of crystalline ZnS fall in the terahertz frequency band.[15−17] Thus, THz-TDS is an advantageous approach to study the detailed low-frequency optical and dielectric properties of ZnS nanoparticles.

In this article, the far-IR optical properties and complex dielectric function of ZnS nanoparticles are experimentally characterized by use of the THz-TDS technique. The measured refractive index, power absorption, and complex dielectric function are compared with the effective medium approach. In the scope of the frequency range from 0.3 to 3.0 THz, the experimental data agree well with the theoretical fit. The THz-TDS measurements indicate that the absorption in ZnS nanoparticles is characterized by a low-frequency lattice vibration localized at 11.6 ± 0.2 THz. The measured power absorption and refractive index are compared with the data of single-crystalline ZnS. The differences of phonon modes between single-crystal ZnS and ZnS nanoparticles are discussed.

### II. Experimental Methods and Materials

ZnS nanoparticles were prepared as follows: A four-neck flask was charged with 100 mL of deionized water and 0.5 g of poly(vinyl alcohol) and was stirred under $N_2$ for 1.5 h. An

* To whom correspondence should be addressed. Tel: (405) 744-7297. Fax: (405) 744-9198. E-mail: wwzhang@okstate.edu.
[†] Shanghai Institute of Applied Physics.
[‡] Oklahoma State University.
[§] Nomadics, Inc.

10.1021/jp055838t CCC: $33.50 
Published on Web 01/12/2006

aqueous solution of 1.6 g of $Na_2S$ and an aqueous solution of 6 g of $Zn(NO_3)_2 \cdot 6(H_2O)$ were prepared and added to the first solution simultaneously via two different necks at the same rate. After the addition, the resulting solution was stirred constantly under $N_2$ at 80 °C for 5 h, and a transparent colloid of ZnS was formed. The nanoparticles were separated from solution by centrifugation and then dried in a vacuum at 50 °C. The identity, crystallinity, crystal structure, and size of the nanoparticles were examined by powder X-ray diffraction (XRD) which was recorded on an INEL diffractometer using a CPS 120 detector and a monochromatized Cu $K_{\alpha 1}$ ($\lambda = 1.54056$ Å) radiation with Si ($a = 0.543088$ nm) as an internal standard. The XRD measurements demonstrate that the particles prepared have the zinc blende structure (sphalerite). The broad XRD lines are indicative of the small size of the ZnS nanoparticles. From the Debye−Scherrer equation, the average size of the ZnS nanoparticle sample is estimated to be around 3 nm.

Two identical handmade cells with dimensions of 25 mm × 16 mm and spacer thickness of 0.42 mm were employed in the terahertz transmission measurements of ZnS nanoparticles. The cells were made of 636-$\mu$m-thick, high-quality silicon slabs with a p-type resistivity of 20 Ω cm. In the measurements, the sample terahertz pulse was obtained with a p-polarized terahertz beam impinging on the cell containing ZnS nanoparticles at normal incidence while the empty cell served as a reference.

The ZnS nanoparticles were characterized by use of a photoconductive switch-based THz-TDS system, in which four parabolic mirrors were arranged in an 8-F confocal geometry.[17] While this configuration enables an excellent beam coupling between the transmitter and the receiver, a frequency-independent 3.5-mm-diameter terahertz beam waist is achieved, which favors the characterization of samples of small dimensions. The THz-TDS system has a useful bandwidth of 0.1 to 4.5 THz (3 mm−67 $\mu$m) and a signal-to-noise ratio (S/N) of >10000:1.[17,18] The transmitted time-domain terahertz pulses and the corresponding spectra of the reference and the ZnS nanoparticles are shown in Figure 1. To increase the S/N, each curve is an average of six individual measurements. The peak amplitude of the sample spectrum is reduced by about 5% due to the frequency-dependent absorption of the ZnS nanoparticles.

The refractive index and power absorption of the ZnS nanoparticles are extracted based on the transmitted terahertz pulses. Because of the clear separation in the time domain between the transmitted and the first reflected pulses, the multiple reflection effect of the sandwiches is ignored in the data analysis. The complex transmission spectra of the reference $E_r(\omega)$ and the sample $E_z(\omega)$ are given by

$$E_r(\omega) = E_{in}(\omega) t_{sa} t_{as} (ik_0 d) \quad (1)$$

$$E_z(\omega) = E_{in}(\omega) t_{sz} t_{zs} (ikd)(-\alpha d/2) \quad (2)$$

where $E_{in}(\omega)$ is the incident pulse spectrum, $k_0 = 2\pi/\lambda_0$ and $k = 2\pi n_z/\lambda_0$ are the wave vectors for the air and the sample, respectively, $n_z$ is the refractive index of ZnS nanoparticles, $d$ is the sample thickness, $\lambda_0$ is the free-space wavelength, $\alpha$ is the power absorption coefficient of ZnS nanoparticles, and $t_{sa}$, $t_{as}$, $t_{sz}$, and $t_{zs}$ are the Fresnel transmission coefficients of terahertz pulses propagating through the Si−air, air−Si, Si−ZnS, and ZnS−Si interfaces, respectively, which are given by $t_{sa} = 2n_s/(1 + n_s)$, $t_{as} = 2/(1 + n_s)$, $t_{sz} = 2n_s/(n_s + n_z)$, and $t_{zs} = 2n_z/(n_s + n_z)$. The $t_{sz}$ and $t_{zs}$ are the complex, frequency-dependent coefficients related to ZnS nanoparticles.

The single-crystal ZnS is an undoped, 10 mm × 10 mm × 1-mm-thick, ⟨100⟩ free-standing crystal grown at temperature of 1100−1250 °C using the seeded vapor-phase free growth technology (RMT Ltd, Russia). Growth was along the ⟨111⟩ direction, and the crystal consists of a 96−98% zinc blende structure and only a 2−4% Wurtzite structure. The resistivity of the crystal is in the range of $10^8$−$10^{12}$ Ω cm. In the THz-TDS measurements, the ZnS crystal is attached to an aluminum holder and centered over a 4.5-mm-diameter hole in the plate, which defines the optical aperture. Another identical clear hole is used to take the reference terahertz pulse. Figure 2 shows the measured transmitted terahertz pulses and the corresponding spectra of the reference and the single-crystal ZnS.

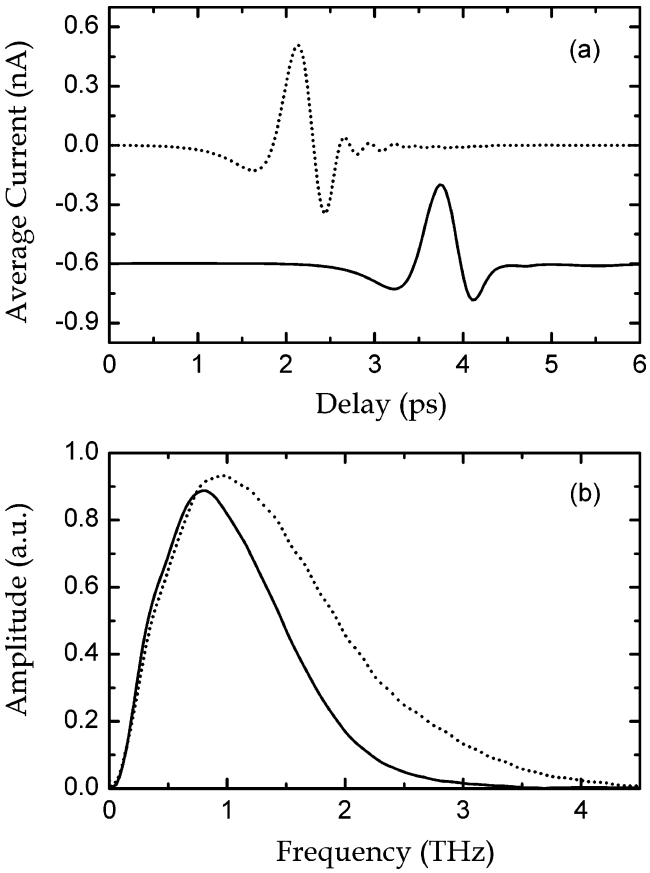


**Figure 1.** (a) Measured transmitted THz pulses through the reference (dotted curve) and the ZnS nanoparticles (solid curve). For clarity, the curves are vertically displaced. (b) The corresponding Fourier transformed amplitude spectra.

## III. Results and Discussions

The frequency-dependent absorption and dispersion of the sample were obtained using the Fourier analysis of the input and output pulses without using the Kramers−Kronig relationship. The real refractive index $n_r$ was obtained directly using the phase difference between the input and the output pulses as mentioned above. The open circles in Figure 3 represent the measured power absorption and refractive index, respectively, as a function of frequency varying from 0.3 to 3.0 THz. As can be seen, the measured power absorption increases with increasing frequency, whereas the measured refractive index $n_r$ approaches a constant 1.5. No prominent absorption peaks are observed, which is an indication that no remarkable change occurs in the refractive index. The fluctuation feature shown in the absorption curve above 2.8 THz arises from the insufficient terahertz power and the increasing absorption of nanoparticles at higher frequencies. The frequency-dependent effective complex dielectric response of ZnS nanoparticles is determined by

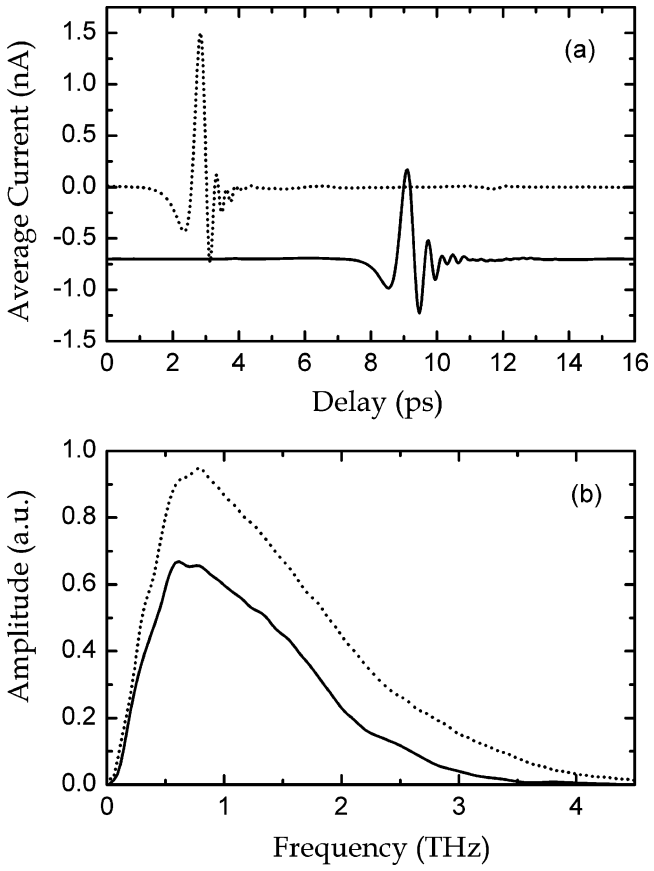


**Figure 2.** (a) Measured transmitted THz pulses through the reference (dotted curve) and the single-crystal ZnS (solid curve). For clarity, the curves are vertically displaced. (b) The corresponding Fourier transformed amplitude spectra.

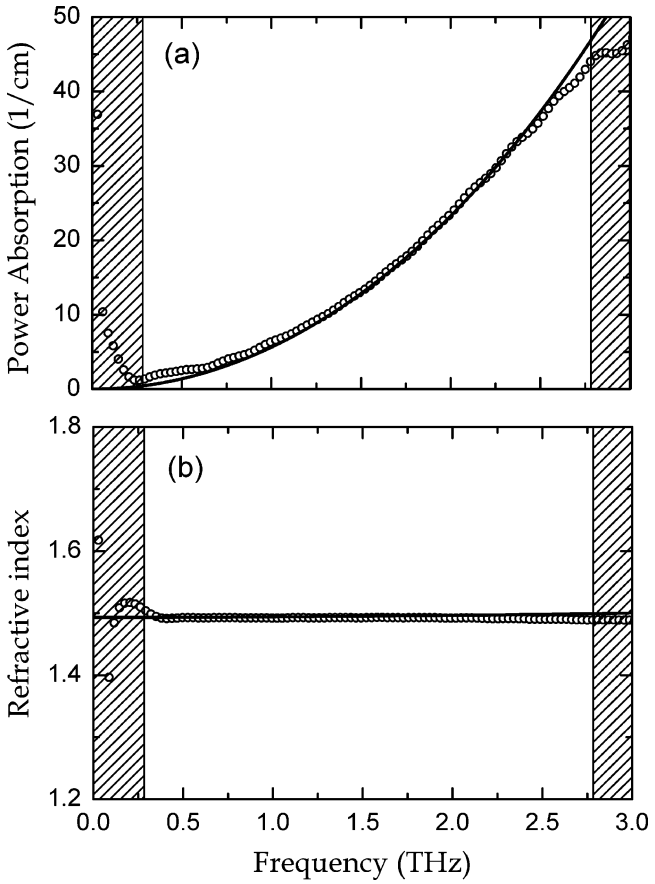


**Figure 3.** (a) Comparison of measured power absorption α (open circles) with that obtained from EMA fitting (solid curve). (b) Measured refractive index (open circles) and the theoretical fitting (solid curve). The measured data may not be accurate in the shaded areas.

the recorded data of power absorption and refractive index through the relationship: $\epsilon(\omega) = (n_r + in_i)^2$, while the imaginary part of the refractive index $n_i$ is related to the power absorption as $n_i = \alpha\lambda_0/4\pi$. As a result, the real and the imaginary part of the dielectric function are given as $\epsilon_r = n_r^2 - (\alpha\lambda_0/4\pi)^2$ and $\epsilon_i = \alpha n_r\lambda_0/2\pi$, respectively.[17] The open circles in Figure 4 illustrate the measured complex dielectric constant.

Generally, for a perfect semiconductor crystal, optical absorption in the far-IR terahertz region is attributed to the lattice vibrations. The interaction of a radiation field with the fundamental lattice vibration results in absorption of electromagnetic waves due to the creation or annihilation of lattice vibration. The phonons are coupled through damping terms of the potential. Part of the energy transferred from the incident radiation field to the transverse optical (TO) mode is transferred to the other phonons. When considering the transverse optical phonon absorption, we usually induce a damping frequency $\gamma$ in a first approximation. According to the Lorentz dispersion theory combined with Huang equations, the dielectric response for a semiconductor crystal usually can be described within the frame of the classical theory of the independent pseudo-harmonic model as[19]

$$\epsilon(\omega) = \epsilon_\infty + \frac{\epsilon_{st}\omega_{TO}^2}{\omega_{TO}^2 - \omega^2 - i\gamma\omega} \quad (1)$$

where $\epsilon_\infty$ is the high-frequency dielectric constant, $\epsilon_{st}$ is the oscillator strength, $\omega_{TO}$ is the frequency of the transverse optical mode, and $\gamma$ is the damping constant. However, as discussed above, the ZnS nanoparticle sample is a complex system in which the ZnS nanoparticles are embedded in air medium. Hence, what we measured is a frequency-dependent effective complex dielectric constant $\epsilon_{eff}$. Therefore, the contribution of the continuous host medium to the dielectric function of ZnS nanoparticles needs to be considered.

Here, we employ the simple effective medium approach (EMA) in the analysis of the dynamic response of ZnS nanoparticles[20,21]

$$\epsilon_{eff}(\omega) = f\epsilon_m(\omega) + (1 - f)\epsilon_h \quad (2)$$

where the filling factor $f$ defines the volume fraction of the particles, $\epsilon_{eff}$ is the effective complex dielectric function of the complex ZnS nanoparticle system, and $\epsilon_h$ and $\epsilon_m$ are the dielectric constants of host medium and pure ZnS nanoparticles, respectively. Usually, the EMA is used to describe the dielectric constant of the structures for which metal or semiconductor particles are embedded in a continuous insulating medium. Here, since the ZnS nanoparticles are filled with air, the dielectric constant of the host medium is $\epsilon_h = \epsilon_{air} = 1.0$. The dielectric function of the pure nanoparticles $\epsilon_m(\omega)$ can be determined by the pseudo-harmonic model with eq 1 considering the phonon contribution to the dielectric function.

First, $\epsilon_m(\omega)$ is calculated by the pseudo-harmonic model of eq 1, which can be written as a set of separate equations that include the real and the imaginary part of the frequency-dependent dielectric function

$$\epsilon_m(\omega) = \epsilon_{rm}(\omega) + i\epsilon_{im}(\omega) \quad (3)$$

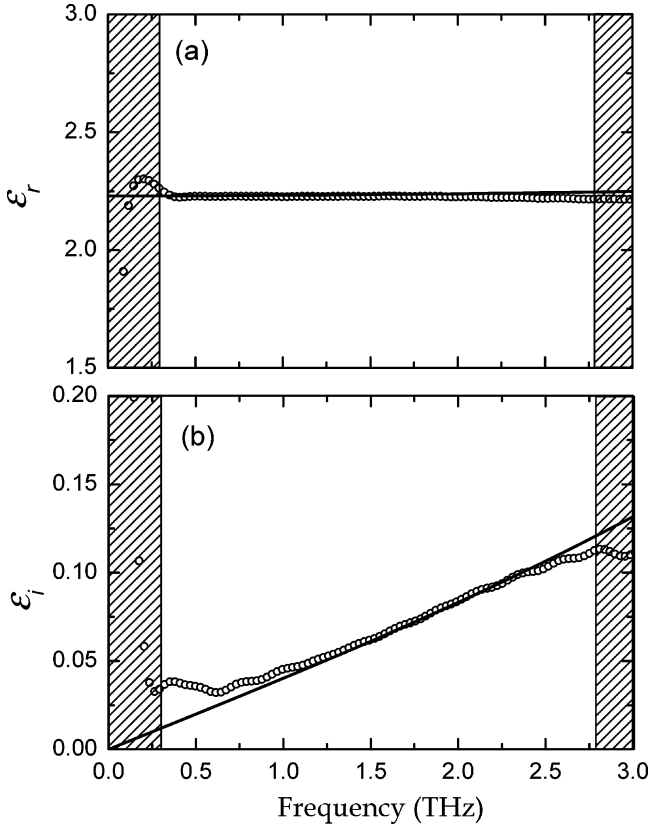


**Figure 4.** Complex dielectric constant of ZnS nanoparticles: (a) measured real part of dielectric constant $\epsilon_r$ (open circles) and the theoretical fitting (solid curve); (b) measured imaginary dielectric constant $\epsilon_i$ (open circles) and the theoretical fitting (solid curve).

where

$$\epsilon_{rm}(\omega) = \epsilon_\infty + \frac{\epsilon_{st}(\omega_{TO}{}^2 - \omega^2)\omega_{TO}{}^2}{(\omega_{TO}{}^2 - \omega^2)^2 + \gamma^2\omega^2} \quad (4)$$

$$\epsilon_{im}(\omega) = \frac{\epsilon_{st}\omega\gamma\omega_{TO}{}^2}{(\omega_{TO}{}^2 - \omega^2)^2 + \gamma^2\omega^2} \quad (5)$$

Next, the effective dielectric function $\epsilon_{eff}$ of the ZnS nanoparticles is calculated using eq 2. As shown by the solid curves in Figures 3 and 4, the measured power absorption, index of refraction, and the corresponding complex dielectric constant are well reproduced for $\epsilon_h = 1.0$, $\epsilon_\infty = 3.0$, $\epsilon_{st} = 2.10$, $\omega_{TO}/2\pi = 11.60$ THz, and $\gamma/2\pi = 8.50$ THz. The filling factor $f = 0.30$ is a measured parameter in the experiments. The damping constant $\gamma$ stands for the line width of the TO phonon absorption peak; the line shape of the fitted TO phonon absorption is quite sensitive to the value of $\gamma$. The good agreement between the measured data and the fitting indicates the presence of a dominant TO phonon resonance centered at $\omega_{TO}/2\pi = 11.6 \pm 0.2$ THz with a line width of $\gamma/2\pi = 8.50$ THz and a strength of $\epsilon_{st} = 2.10$. Such a TO phonon resonance is quite consistent with the previously reported characteristic vibration frequency $11.6 \pm 0.4$ THz.[22] In comparison, this value is greater than the characteristic phonon frequency of bulk ZnS, $7.12 \pm 1.2$ THz.[22]

As mentioned above, the optical properties of nanoparticles can differ from those of their single crystal or bulk form due to the surface effect because of their finite size. Hence, it is essential to compare the THz spectroscopic response of ZnS nanoparticles with that of single-crystal ZnS. Figure 5 shows a comparison of the experimentally extracted power absorption and refractive index of single-crystal ZnS with that of ZnS nanoparticles. The single-crystal ZnS shows lower absorption, while the refractive index of single-crystal ZnS is increased. In addition, two prominent phonon resonances, located at 2.20 and 2.80 THz, for single-crystal ZnS are observed as a further distinction. These characteristic phonon frequencies are assigned to TA(L) = 73 $cm^{-1}$ (2.2 THz)[23] and TA(X) = 93 $cm^{-1}$ (2.8 THz), respectively.[24] The fit on the measured data indicates that a TO phonon resonance is localized at $8.13 \pm 0.2$ THz,[17,25] which is consistent with the reported characteristic phonon frequency of $7.12 \pm 1.2$ THz.[22]

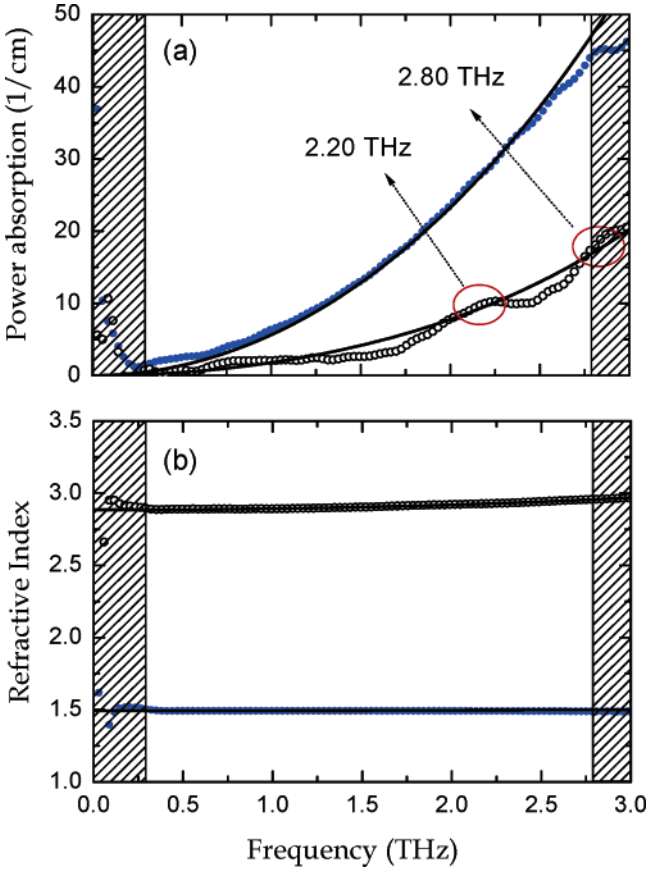


**Figure 5.** Comparison of measured (a) power absorption and (b) refractive index of ZnS nanoparticles (solid circles) with that of single-crystal ZnS (open circles). The solid curves are the theoretical fit on the experimental data.

Generally, for particles, the resonance peaks of optical phonons shift to higher frequency as the particle size decreases. For optical phonons in nonpolar microcrystals such as Si and Ge, size-dependent shift and broadening were commonly observed.[5,26] In addition, the Raman peak of Ag particles was observed to shift to a higher frequency as the particle size decreased.[6] These features provide a qualitative explanation of our observed result that the TO frequency of ZnS nanoparticles is higher than that of single-crystal ZnS. The phonon modes of single-crystal ZnS at 2.2 and 2.8 THz are not found in the spectra of ZnS nanoparticles. Table 1 summarizes the phonon dispersion for ZnS nanoparticles and single-crystal ZnS based on our measured data. For ionic crystalline solids, such as single-crystal ZnS, the atoms are bound in periodic arrays which propagate waves with constraints and behaviors imposed by the dynamics of lattice motion. The interaction of a radiation field with the fundamental lattice vibrations generally results in the absorption of electromagnetic waves due to the creation or annihilation of lattice vibrations. Optical absorption of ionic

**TABLE 1: Comparison of the Observed and Predicted Characteristic Phonons of Single-Crystal ZnS and ZnS Nanoparticles**

| sample | TA(X) | TA(L) | TO(Γ) |
|---|---|---|---|
| ZnS crystal | 2.20 THz[a] | 2.80 THz[b] | 8.13 THz[c] |
| ZnS nanoparticles | | | 11.60 THz[d] |

[a] Consistent with results reported previously in ref 23. [b] Consistent with results reported previously in ref 24. [c] Consistent with results reported previously in ref 25. [d] Consistent with results reported previously in ref 22.

crystals in the far-IR region can be ascribed to the lattice vibration, which includes many modes induced by the interaction between metal ions and anions, as well as interaction between metal ions and between anions. However, as discussed above, the surface-to-volume ratio of nanoparticles is very large and the number of atoms on the surface is comparable to or larger than the number of atoms inside the particle. The absorption is mainly ascribed to the contribution of the surface of the particles. Therefore, it is not surprising that not all resonance modes of bulk ZnS are observed in ZnS nanoparticles. The experimental results clarify that the acoustic phonons become confined in small-size nanoparticles compared to bulk materials. Due to the localization of acoustic vibrational motion, the TA(L) and the TA(X) modes in single-crystal ZnS are not observed in ZnS nanoparticles. Our measurements are also in good agreement with the previous experimental report.[14,27,28]

## IV. Conclusions

A far-IR THz-TDS study of the dielectric and optical properties of ZnS nanoparticles has resolved the characteristic phonon resonance process. The EMA-based theoretical fit indicates that the characteristic phonon resonance of ZnS nanoparticles is dominated by the TO phonon at 11.6 THz, which is quite consistent with the previous report. This characteristic phonon frequency is higher than that of single-crystal ZnS. Furthermore, we demonstrate that not all the phonon modes in single-crystal ZnS are observed in ZnS nanoparticles because the acoustic phonons of the ZnS nanoparticle become confined. These features are clearly related to the size effect in ZnS nanoparticles.

**Acknowledgment.** The authors acknowledge the exceptional efforts of Jianming Dai and Mingxia He. This work was partially supported by the Oklahoma EPSCoR for the National Science Foundation.

## References and Notes

(1) Meng, X.-M.; Jiang, Y.; Liu, J.; Lee, C.-S.; Bello, I.; Lee, S.-T. *Appl. Phys. Lett.* **2003**, *83*, 2244.
(2) Wang, Y.; Herron, N. *J. Phys. Chem.* **1991**, *95*, 525.
(3) Suyver, J. F.; Wuister, S. F.; Kelly, J. J.; Meijerink, A. *Nano Lett.* **2001**, *1*, 429.
(4) Zhu, Y.; Yuan, C. L.; Onga, P. P. *J. Appl. Phys.* **2002**, *92*, 6928.
(5) Sasaki, Y.; Horie, C. *Phys. Rev. B* **1995**, *47*, 3811.
(6) Fujii, M.; Nagareda, T.; Hayashi, S.; Yamamoto, K. *Phys. Rev. B* **1991**, *44*, 6243.
(7) Tan, M.; Cai, W.; Zhang, L. *Appl. Phys. Lett.* **1997**, *71*, 3697.
(8) Geng, B. Y.; Zhang, L. D.; Wang, G. Z.; Xie, T.; Zhang, Y. G.; Meng, G. W. *Appl. Phys. Lett.* **2004**, *84*, 2157.
(9) Gupta, S.; Meclure, J. S.; Singh, V. P. *Thin Solid Films* **1997**, *33*, 299.
(10) Yoffe, D. *Adv. Phys.* **2001**, *50*, 1.
(11) Murray, C. B.; Norris, D. B.; Bawendi, M. G. *J. Am. Chem. Soc.* **1993**, *115*, 8706.
(12) Haggata, S. W.; Li, X.; Cole-Hamilton, D. J.; Fryer, J. R. *J. Mater. Chem.* **1996**, *6*, 1771.
(13) Murakoshi, K.; Hosokawa, H.; Tanaka, N.; Saito, M.; Wada, Y.; Sakata, T.; Mori, H.; Yanagida, S. *Chem. Commun.* **1998**, *3*, 321.
(14) Xu, J.; Mao, H.; Sun, Y.; Du, Y. *J. Vac. Sci. Technol., B* **1997**, *15*, 1465.
(15) Hattori, T.; Homma, Y.; Mitsuishi, A.; Tacke, M. *Opt. Commun.* **1973**, *7*, 229.
(16) Vagelatos, N.; Wehe, D.; King, J. S. *J. Chem. Phys.* **1974**, *60*, 3613.
(17) Thamizhmani, L.; Azad, A. K.; Dai, J.; Zhang, W. *Appl. Phys. Lett.* **2005**, *86*, 131111.
(18) Zhang, J.; Grischkowsky, D. *J. Phys. Chem. B* **2004**, *108*, 18590.
(19) Balkanski, M. *Optical Properties of Solids*; Abelès, F., Ed.; North-Holland: New York, 1972; Chapter 8.
(20) Weissker, H.-Ch.; Furthmuller, J.; Bechstedt, F. *Phys. Rev. B* **2003**, *67*, 165332.
(21) Fratini, S.; de Pasquale, F. *Phys. Rev. B* **2001**, *63*, 153101.
(22) Gilbert, B.; Huang, F.; Zhang, H.; Waychunas, G. A.; Banfield, J. F. *Science* **2004**, *305*, 651.
(23) Feldkamp, L. A.; Venkatamaran, G.; King, J. S. *Solid State Commun.* **1969**, *7*, 1571.
(24) Marschall, R.; Mitra, S. *Phys. Rev.* **1964**, *A 134*, 1019.
(25) Balkanski, M.; Nusimovici, M.; Le Toullec, T. *J. Phys (Paris)* **1964**, *25*, 305.
(26) Richter, H.; Wang, Z. P.; Ley, L. *Solid State Commun.* **1981**, *39*, 625.
(27) Nomura, S.; Kobayashi, T. *Solid State Commun.* **1992**, *82*, 335.
(28) Cerullo, G.; Silvestr, S. D.; Banin, U. *Phys. Rev. B* **1999**, *60*, 1928.